

# L-Methioninase as a Selective Anticancer Agent: Dose-Dependent Cytotoxicity and Metastasis Suppression in Methionine-Dependent Tumor Cells

Abbas Abed Noor Al-Owaidi\*, Mohammed Abdullah Jebor

Department of Biology, College of Sciences, University of Babylon, Babylon, Hillah, 51001, Iraq

Received: Jan. 2025; Accepted: Mar. 2025

**Abstract-** L-methioninase (L-Met), a methionine-degrading enzyme, has shown potential for anticancer therapy. Many tumor tissues have a limited ability to produce methionine and depend on external sources; hence, these tumors can be targeted by methionine-based treatments. The present study was conducted to investigate the effects of L-Met on cancer cells, particularly hepatocellular carcinoma (HepG2) and pancreatic carcinoma (PANC-1), and to evaluate its viability as a therapeutic agent. Various techniques, including ammonium sulfate precipitation, dialysis, ion-exchange chromatography, and gel filtration chromatography, were employed to purify the enzyme L-Met. A cytotoxicity test was conducted against HepG2 and PANC-1 cells (at 25-200 µg/mL concentrations), using the MTT to evaluate cell viability, total nuclear intensity (TNI), and cell membrane permeability (CMP). Statistical analysis was done using one-way ANOVA and Dunnett's multiple comparisons test to compare study groups. L-Met displayed dose-dependent growth inhibition of the specified cell lines. The PANC-1 cell line exhibited an  $IC_{50}$  of 64.68 µg/mL, indicating a higher sensitivity to L-Met compared to WRL 68 normal cells, which had an  $IC_{50}$  of 214.0 µg/mL. Regarding HepG2, an even lower  $IC_{50}$  of 66.44 µg/mL was observed, further confirming the selective targeting of cancer cells by L-Met. Treatment with L-Met at a 200 µg/mL concentration significantly decreased TNI and CMP levels in both the PANC-1 and HepG2 cell lines, indicating increased cytotoxicity and compromised membrane integrity. Additionally, L-Met reduced matrix metalloproteinase activities in both cancer cell lines, a critical factor in metastasis. Our study demonstrates the dose-dependent cytotoxic effects of L-Met on methionine-dependent tumor cells, specifically HepG2 and PANC-1. These findings highlight the need for optimized L-Met dosing strategies in cancer treatment, particularly for methionine-dependent malignancies, paving the way for its potential use in targeted cancer therapy.

© 2025 Tehran University of Medical Sciences. All rights reserved.

*Acta Med Iran* 2025;63(March-April):83-97.

<https://doi.org/10.18502/acta.v63i2.18962>

**Keywords:** L-methioninase; *Pseudomonas aeruginosa*; Hepatocellular carcinoma; Pancreatic carcinoma

## Introduction

L-methioninase (L-Met) catalyzes the breakdown of L-methionine into ammonia,  $\alpha$ -ketobutyrate, and methanethiol. Pyridoxal 5'-phosphate is essential for the enzyme to eliminate L-methionine in its  $\gamma$  form (1), as well as L-cysteine and its analogs in their  $\alpha$  and  $\beta$  forms (2).

Methionine is an essential amino acid crucial to mammalian metabolism, including protein synthesis, glutamine production, and polyamine biosynthesis (3,4).

Several cancer cells exhibit an increased dependence on plasma methionine for the synthesis of protein and regulation of DNA expression (5). Deprivation of methionine has been shown to induce apoptosis in cancer cells and arrest them in the late S-G2 phase of the cell cycle (CC) (6).

One promising approach in anticancer therapy involves using L-Met to inhibit the growth of tumors that are dependent on L-methionine for their growth and proliferation (5). Numerous cancer cell lines, including those derived from the breast, kidney, colon, lung, and

**Corresponding Author:** A.A.N. Al-Owaidi

Department of Biology, College of Sciences, University of Babylon, Babylon, Hillah, 51001, Iraq  
Tel: +9647705713626, E-mail address: alowaidiabbas47@gmail.com

Copyright © 2025 Tehran University of Medical Sciences. Published by Tehran University of Medical Sciences

This work is licensed under a Creative Commons Attribution-NonCommercial 4.0 International license (<https://creativecommons.org/licenses/by-nc/4.0/>). Non-commercial uses of the work are permitted, provided the original work is properly cited

## **L-methioninase in methionine-dependent cancer therapy**

prostate tissues, have been used to assess the anticancer activity of L-Met (7). Recombinant methioninase has demonstrated broad selective efficacy against various cancer cell lines in vitro (7). It is also effective against the BRAF-V600E mutant melanoma patient-derived orthotopic xenografting in a mouse model (8). Sundar and Nellaiah found that administering L-Met to mice with Dalton's ascites lymphoma cell lines inhibited tumor growth and increased the longevity of the mice (9).

Human cancer cell lines and cancer xenografts have displayed a dependency on methionine in animal models, indicating that cancer cells require higher levels of methionine for their development compared to normal cells (10,11). This metabolic abnormality is specific to cancer cells, preventing them from proliferating in media with low methionine levels. In contrast, non-malignant mammalian cells can divide normally without methionine, as long as homocysteine is available in the growth media (12). Animals fed diets that substitute homocysteine for methionine often exhibit normal development (12). However, in the presence of homocysteine, most cancer cells fail to proliferate and depend on exogenous methionine (13,14). Methionine restriction has a greater effect on tumors than on healthy tissues. Conversely, limiting other essential amino acids proves either ineffective or highly detrimental (15).

The current study was designed to evaluate the effect of L-Met on pancreatic (PANC-1) and hepatocellular (HepG2) cancer cells and to investigate the mechanisms underlying the inhibitory effects of L-Met on cell survival and CC progression.

## **Materials and Methods**

### **Sample preparation**

#### **Sample collection**

A total of 150 clinical samples were randomly collected from patients with urinary tract infections, burns, sputum infections, wounds, and otitis media who were hospitalized at Baghdad Hospital (Iraq). All samples were transferred under sterile and cool conditions.

#### **Buffer preparation**

Potassium phosphate (0.5 M, pH 7), Tris-HCl (0.05 M, pH 7), and Tris-base (0.1 M, pH 8 and 9) buffers were used to maintain a specific pH during the enzyme activity assay. Additionally, we prepared specific solutions for purification, including sodium chloride (0.25 M), sodium hydroxide (0.25 M), and hydrochloric acid (0.25 M).

#### **Isolation and identification of pseudomonas**

### **aeruginosa**

Samples were cultured in brain heart infusion broth and subjected to general and differential culture techniques. *P. aeruginosa* colonies were identified using lactose non-fermenting MacConkey and cetrimide agars for pyocyanin and fluorescein production and the VITEK-2 system. Biochemical tests, including oxidase, catalase, indole, citrate utilization, and urease production confirmed the identification of bacteria.

### **L-met activity assay**

The Nesslerization method was utilized to assess the activity of L-Met. A reaction mixture containing 1% L-methionine, potassium phosphate buffer (0.5 M, pH 7), pyridoxal phosphate (PLP), and crude enzyme was prepared and incubated at 30° C for one hour. The reaction was then stopped by adding trichloroacetic acid, and the release of ammonia was measured using a Nessler reagent. The enzyme-specific activity was expressed as micromoles of ammonia produced per minute per milligram of protein.

### **Protein concentration determination**

Bradford's method was employed to quantify the protein concentration. The absorbance was measured at 595 nm, and a standard curve was generated using bovine serum albumin.

### **Purification of L-met**

#### **Ammonium sulfate precipitation**

The crude enzyme was added to the ammonium sulfate at different concentrations: 30%, 40%, 50%, 60%, 70% and 80%. The enzyme was centrifuged at 6,000 rpm at 4°C for 6 hours. The optimum saturation was then determined to be 70%, at which point the enzyme exhibited maximum activity.

#### **Enzyme dialysis**

A precipitated enzyme was dialyzed using a dialysis tube with a molecular weight cut-off of 3,500 Da against potassium phosphate buffer, at pH 7, maintained at 4° C for 24 hrs.

#### **Ion exchange chromatography**

Further purification of the target was performed by using DEAE-cellulose resin. The enzyme solution was applied to the DEAE-cellulose column and subsequently washed with phosphate buffer. Proteins were eluted with stepwise gradients of sodium chloride at concentrations of 0.1 M and 1 M. Enzyme activity and protein concentration were assessed for each fraction.

### Gel filtration chromatography

In the final step, Sephadex G-150 gel filtration chromatography was performed. The enzyme was applied to a pre-equilibrated column, and fractions were collected. For each enzyme activity, the protein concentration was determined.

### Enzyme characterization

#### Optimum pH and temperature

The optimum pH of L-Met was determined using buffers with pH values ranging from 4 to 9. Also, temperature stability was assessed across a series of temperatures from 10° C to 60° C. Enzyme activity was measured based on substrate degradation under each condition.

### Cytotoxicity assay

#### Cell line culturing

The L-Met cytotoxicity was evaluated on two cancer cell lines: HepG2 and PANC-1. The cells were cultured in RPMI-1640 medium supplemented with 10% fetal bovine serum, 100 IU/mL of penicillin, and 100 µg/mL of streptomycin.

#### MTT assay

Tumor cells were seeded in a 96-well plate at a density of  $1 \times 10^4$ – $1 \times 10^6$  cells/mL and incubated with serial dilutions of the enzyme at concentrations of 25-400 µg/mL for 24 hours. After the incubation period, MTT solution was added to each well, followed by a further incubation of 4 hours. The resultant purple formazan crystals, formed from the reduction process, were dissolved in a solubilization solution and measured at 575 nm using an ELISA reader. The  $IC_{50}$  was calculated based on the enzyme concentration that resulted in 50% inhibition of cell viability.

### VCC and TNI

VCC was utilized to measure the number of living cells present after L-Met treatment. The VCC was assessed using the MTT assay, in which cells were treated with various enzyme concentrations and subsequently incubated with an MTT reagent. The reduction in cell

viability was quantified by measuring MTT to formazan conversion. TNI involves evaluating nuclear damage induced by the enzyme, likely indicating DNA damage or apoptosis. TNI was determined using nuclear staining techniques, e.g. DAPI, and analyzed with a fluorescence microscope to evaluate the extent of nuclear fragmentation, a characteristic feature of apoptosis. In the end, treated cells were compared with untreated cells to assess the effect of L-Met on cell integrity.

### Statistical analysis

The normality of the data was evaluated using the Shapiro-Wilk test. Normally and non-normally distributed data were analyzed using parametric tests and non-parametric tests, respectively. All data were expressed as the mean±standard deviation (SD) or mean±standard error of the mean (SEM). Graphical representations were created to visualize trends and comparisons across various experimental conditions, with error bars indicating the variability within the data. A one-way Analysis of Variance (ANOVA) was conducted to assess the impact of different experimental conditions—such as nitrogen sources, carbon sources, pH, temperature, and incubation duration—on L-Met activity. When significant differences were identified ( $P < 0.05$ ), post-hoc pairwise comparisons were performed using Tukey's Honestly Significant Difference (HSD) test to detect differences between specific groups. A repeated-measures ANOVA was employed for experiments that included time-dependent alterations in enzyme activity (e.g. optimum incubation period). Post-hoc analyses were conducted to identify specific time points with significant differences. The cytotoxicity effects of L-Met on cancer cell lines (A-172 and SK-OV-3) were assessed by determining the VCC, TNI, cell membrane permeability (CMP), and matrix metalloproteinase (MMP) levels. The VCC, TNI, and CMP data were analyzed using Dunnett's Multiple Comparisons Test to compare treated groups with the control group. Results from all experiments were deemed statistically significant if the p-value was less than 0.05. All statistical analyses were performed using GraphPad Prism 9.4 software.

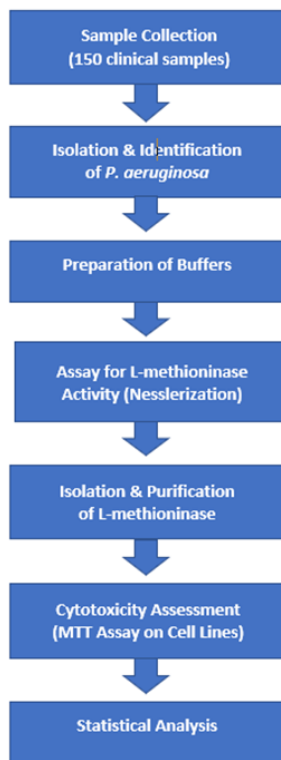


Figure 1. Schematic representation of the study procedure

## Results

### Optimal conditions for producing L-Met

#### Optimal temperature

Temperature stability was observed within the range of 10° C-60° C. Enzyme activity increased with temperature until it reached a maximum of 1.5 U/ml at 37°C. As the temperature continued to rise, enzyme activity declined, reaching 0.9 U/ml and 0.5 U/ml at 42°

C and 47° C, respectively, indicating a reduction in enzyme performance at higher temperatures. The specific activity of the enzyme also increased with rising temperatures, peaking at 37° C with a value of 2.7 U/mg of protein. However, at 42° C, the specific activity of L-Met reduced to 0.9 U/mg of protein, suggesting that enzyme efficiency diminishes with increasing temperature (Figure 2).

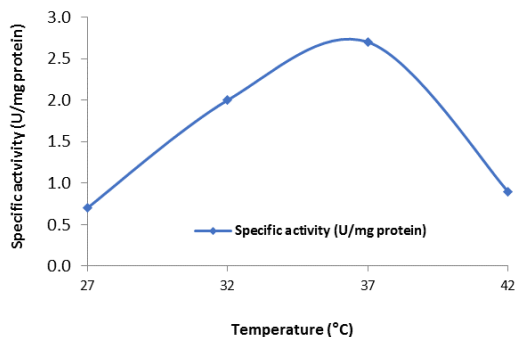


Figure 2. Influence of temperature on the specific activity of L-Met

#### Optimal PH

The optimum pH range for enzyme activity was found

to be between pH 4 and pH 9. At pH 7, the enzyme demonstrated the highest activity, with a significant reduction in activity observed at both more acidic and alkaline pH levels. Also, the data revealed that the stability and activity of the enzyme were highest at pH 7 and 8, though there was a substantial decrease in activity at highly acidic and alkaline pH levels (Figure 3).

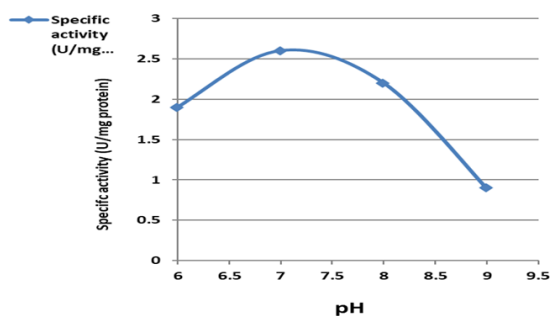


Figure 3. Optimum pH for the production of L-Met enzyme from *Pseudomonas aeruginosa* A6 following incubation at 37°C for 48 h

### Optimal period for incubation

The specific activity of the enzyme increased to a peak of 3.3 U/mg of protein for 48 h. However, after 72 hours, the specific activity of L-Met declined to 2.5 U/mg of protein, indicating a decrease in enzyme efficiency with

prolonged incubation (Figure 4).

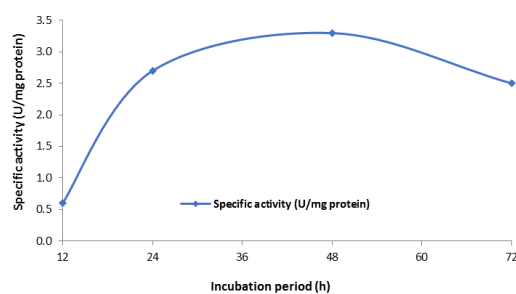


Figure 4. Optimum incubation period for producing L-Met by *Pseudomonas aeruginosa* at 37°C

### Isolation of L-met from *P. aeruginosa*

Three purification steps were used to isolate the enzyme produced by *P. aeruginosa*. The first step included precipitating L-Met with ammonium sulfate. A precipitation range of 30%-80% ammonium sulfate saturation was employed in the crude enzyme solution. The optimum condition for maintaining enzyme activity was observed at 70% ammonium sulfate saturation, yielding the highest enzyme activity of 4.5 U/ml and a specific activity of 11.2 U/mg of protein (Table 1).

Table 1. Activity of L-Met at different ammonium sulfate saturations

Ammonium sulfate (%)	Enzyme activity (U/ml)
30	0.9
40	1.5
50	2
60	4
70	4.5
80	3.8

### Ion-Exchange Chromatography (IEC)

DEAE-cellulose resin was utilized to enhance the purification of the enzyme. After eluting the enzyme fractions using a sodium chloride gradient ranging from 0.1 to 1 M, we evaluated the protein content and activity. IEC separates ionizable molecules based on differences in their charge characteristics. The observed fractions were analyzed by measuring their optical density (OD) at 280 nm with the aid of a spectrophotometer. A distinct protein peak was noted during the washing phase, where a potassium phosphate buffer was used to elute positively charged proteins. This washing process continued until the OD values reached zero, signifying the complete elution of positively charged proteins from the column. A second peak was identified during the elution phase, where a sodium chloride concentration gradient was

applied to release the negatively charged proteins bound to the column. Fractions 59 to 66 contained the majority of enzyme activity, exhibiting a purification fold of 2.6 and an overall yield of 48%. The specific activity of these fractions was determined to be 10.7 U/mg of protein (Figure 5).

### Gel filtration chromatography of L-met

L-Met was successfully purified in the final step using Sephadex G-150 gel filtration. During this process, the obtained fractions were assessed for protein concentration and enzyme activity (Figure 6). The application of Sephadex G-150 gel filtration resulted in a significant increase in the specific activity of the enzyme, achieving a level of 16.6 U/mg, along with a 4.6-fold increase in purity. However, the recovery yield from this

## L-methioninase in methionine-dependent cancer therapy

step relatively reduced at 45%, as compared to other purification techniques (Table 2).

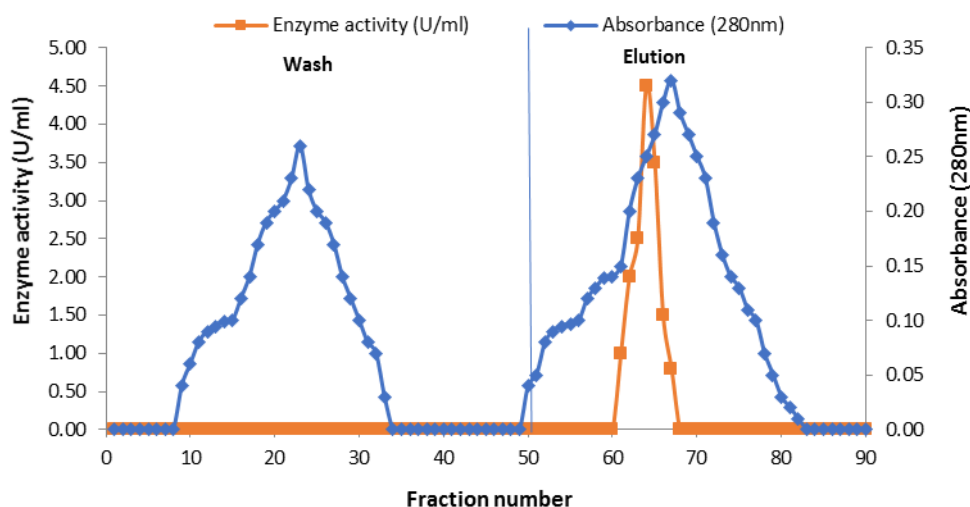


Figure 5. L-Met ion-exchange chromatography using DEAE-cellulose resin

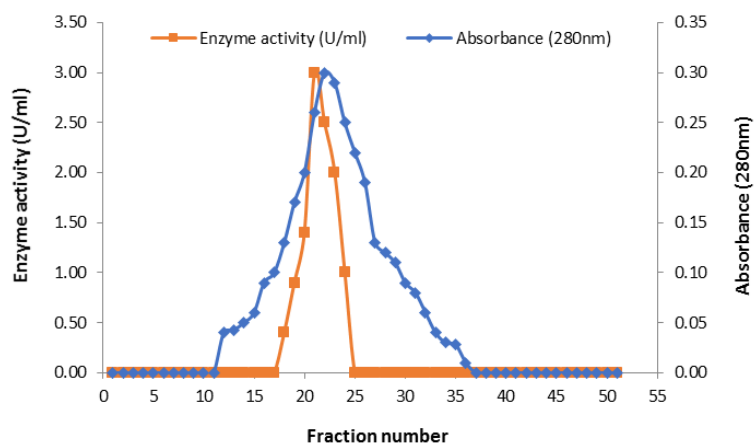


Figure 6. Gel filtration chromatography of L-Met using Sephadex G-150

Table 2. Purification step for L-Met production from *Pseudomonas aeruginosa*

Purification step	Volume (ml)	Enzyme activity (U/ml)	Protein concentration (mg/ml)	Specific activity (U/mg)	Total activity (U)	Purification (folds)	Yield (%)
Crude enzyme	70	1	0.3	3.3	70	1	100
Ammonium sulphate recipitation (70%)	11	4.5	0.4	11.2	49.5	3.4	70.7
DEAE-cellulose	21	2.2	0.1	22	46.2	6.6	66
Sephadex- G150	21	1.5	0.09	16.6	31.5	5	45

### Characterization of purified L-met Effect of PH on the activity and stability of L-met

The correlation of pH levels with enzyme activity, measured in U/ml, is depicted in Figure 7. The enzyme

exhibited optimum activity at a pH close to 7, reaching a maximum activity level of 1.5 U/ml. However, enzyme activity reduced under both more acidic (pH 5) and more alkaline (pH 9) conditions. Also, enzyme activity

gradually declined at higher alkaline (pH 9 and 10) and acidic (pH 5) pH levels, with optimal structural stability observed at pH 7 and 8.

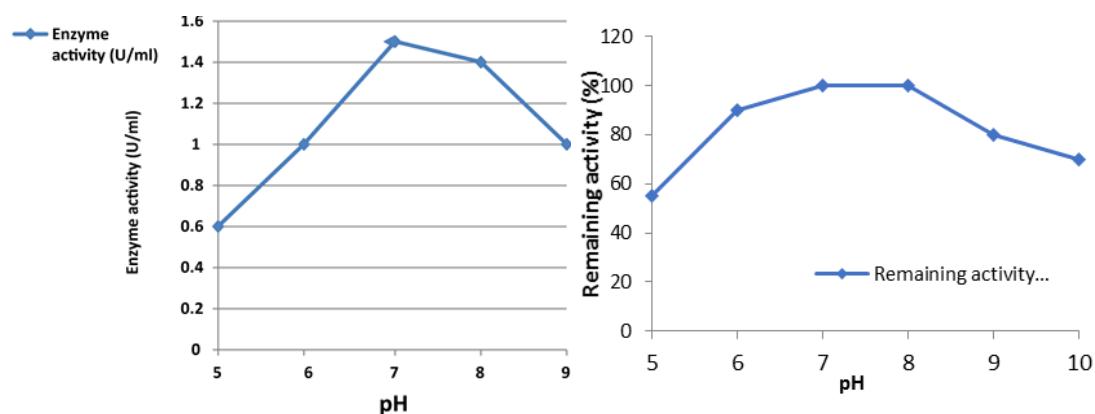


Figure 7. Effect of pH on the (a) specific activity and (b) structural stability of enzyme

### Effect of temperature on the activity and stability of enzyme

The correlation of temperature with enzyme activity, measured in U/ml, is illustrated in Figure 8. The enzyme demonstrates optimum activity at 37° C. At this temperature, the specific activity of the enzyme reached its peak, followed by a decline at both lower and higher temperatures. The percentage of residual enzyme activity in Figures 3-13 displays the structural stability of the

enzyme across varying temperatures. The highest structural stability was observed at 32° C and 37° C. However, when the temperature exceeded 37° C, there was a significant decrease in enzyme stability, with notable reductions in enzyme activity recorded at temperatures above 42° C. This observation indicates that elevated temperatures compromise the structural integrity of the enzyme, with optimal stability occurring between 32° C and 37° C.

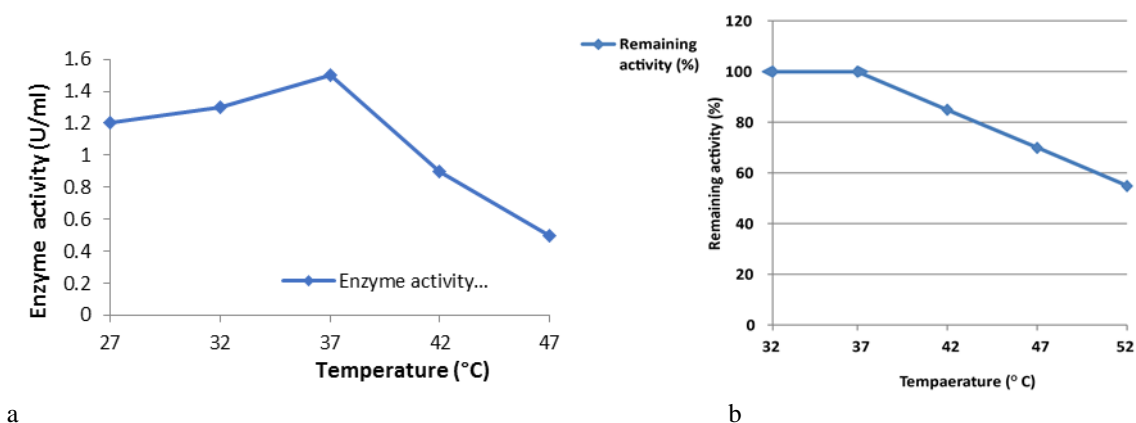


Figure 8. a) Optimal temperature for (a) specific activity and (b) structure stability of enzyme

### Evaluation of L-met purity

Using polyacrylamide gel electrophoresis, we evaluated the purity of L-Met isolated from *P. aeruginosa*. Following the gel filtration process, the analysis of the protein profile displayed a single band, suggesting that the enzyme had attained a high level of

purification. The molecular weight of the isolated L-Met was found to be around 55 kDa.

### Effect of ionic factors on the activity of L-met

The activity of L-Met was evaluated using the Nesslerization technique. The reaction mixture, which

## L-methioninase in methionine-dependent cancer therapy

included potassium phosphate buffer, 1% L-Met, crude enzyme, and PLP, was incubated at 30° C for one hour. After the reaction was terminated, the Nessler reagent was added to measure the release of ammonia. The specific activity of the enzyme was calculated in terms of micromoles of ammonia produced per minute per milligram of protein. The residual activity of L-Met following exposure to different ionic compounds at a concentration of 5 mM is represented in Table 3. The control enzyme indicated 100% activity. Exposure to

NaNO<sub>3</sub> and CuCl<sub>2</sub> led to a reduction of enzyme activity to 70%, reflecting a mild inhibitory effect. Conversely, CaCl<sub>2</sub> maintained 90% residual activity, implying only a slight inhibition. Both MnCl<sub>2</sub> and KCl did not affect enzyme activity, preserving 100% residual activity. These findings suggest that certain salts, such as MnCl<sub>2</sub> and KCl, do not inhibit L-Met activity, while others, including NaNO<sub>3</sub> and CuCl<sub>2</sub>, exhibit a mild inhibitory effect.

**Table 3. Effect of various reagents on L-Met activity**

Reagent	Concentration (mM)	Remaining activity (%)
Control (enzyme)		100
NaNO <sub>3</sub>	5	70
CaCl <sub>2</sub>	5	90
CuCl <sub>2</sub>	5	70
MnCl <sub>2</sub>	5	100
KCl	5	100

### Cytotoxicity effect of L-met on cancer cell lines Hepatocellular cell line (HepG2)

In the present study, we examined the various effects of L-Met on the human hepatocellular cell line HepG2. To assess the effect of different treatment concentrations of L-Met, we applied doses 200, 100, 50, and 25 µg/mL. We also utilized the Dunnett's multiple comparison test to evaluate cell viability across the various experimental conditions (Figure 9).

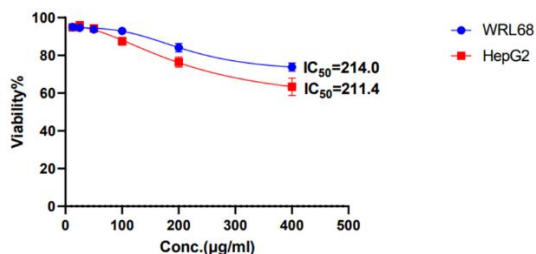


**Figure 9.** L-Met treatment dose-response curves produced for the normal liver cell line WRL68 and the HepG2 cell line. Cell viability was assessed after a 24-hour exposure to varying doses of L-Met (25–500 µg/mL). The calculated IC<sub>50</sub> values showed that the HepG2 cancer cell line is more susceptible to the effects of L-Met than the WRL68 normal cell line, with IC<sub>50</sub> values of 214.0 µg/mL for WRL68 and 66.44 µg/mL for HepG2. Standard deviations from trials conducted in triplicate are represented by error bars

In the HepG2 cell line, a decrease in the viable cell count (VCC) was observed as the dose of L-Met increased. The treatments at 200 µg/mL resulted in significantly lower viability when compared to the untreated control, with an average difference of 1971

( $P=0.0022$ ). The 100 µg/mL dose also demonstrated a substantial decrease in VCC, showing an average difference of 1469 ( $P=0.0082$ ). In contrast, the lower concentrations of 50 and 25 µg/mL did not indicate significant differences, with p-values of 0.8553 and  $>0.9999$ , respectively. These results indicate that higher doses of L-Met have a pronounced effect, while lower doses are insufficient to induce a cytotoxic response in osteoblastoma cells (Figure 10).

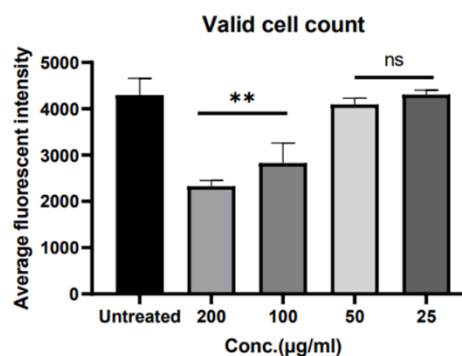


**Figure 10.** L-Met enzyme tested for its effect on VCC permeability by assessing the fluorescent intensity

We observed a similar trend in the HepG2 cell line regarding TNI. The specific dose of L-Met at 200 µg/mL resulted in a significant reduction compared to the vehicle control, with a mean difference of -215.5 ( $P=0.0007$ ). In contrast, the 100 µg/mL dose of L-Met produced a mean difference of -151.0 ( $P=0.0034$ ). However, the concentrations of 50 and 25 µg/mL did not induce any significant reductions in cell viability, as indicated by

their respective p-values of 0.3358 and 0.9922. These data further support the dose-dependency cytotoxicity of L-Met in the HepG2 cell line (Figure 11).

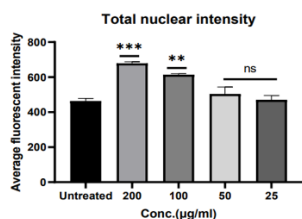


**Figure 11.** L-Met enzyme tested for its effect on TNI permeability by assessing the fluorescent intensity

Further analysis also indicated a significant difference in CMP. The 200 µg/mL dose exhibited a mean difference of -59.00, with statistical significance at  $P=0.0092$ , indicating a substantial decrease in CMP in HepG2 cells. In contrast, the results for the lower doses of 100, 50, and 25 µg/mL were not statistically significant, as their respective p-values were above 0.05 (Figure 12).

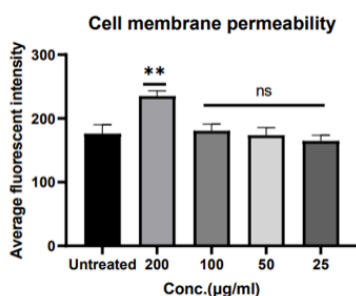


**Figure 12.** L-Met enzyme tested for its effect on CMP by assessing the fluorescent intensity

The dose of 200 µg/mL significantly reduced MMP with a mean difference of 279.0 ( $P=0.0037$ ) and for 100 µg/mL as 158.5 and  $P=0.0392$ . Once again, the two lowest concentrations of 50 and 25 µg/mL did not reveal any significant effect, further establishing that a higher concentration is necessary for the expression of cytotoxicity in these two cell lines (Figure 13).

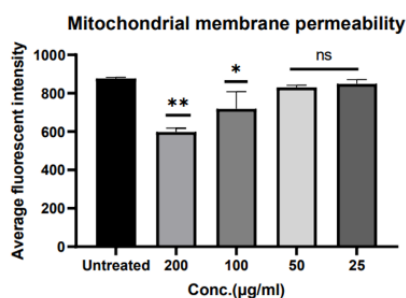


**Figure 13.** L-Met enzyme tested for its effect on MMP by assessing the fluorescent intensity

The analysis of the CC further confirmed these dose-dependent trends. The 200 µg/mL dose for the HepG2 cell line exhibited a significant decrease, with a mean difference of -104.5 and a p-value of 0.0015. In contrast, the 100 µg/mL dose also resulted in a decrease in CC progression, with a mean difference of -64.50 and a  $P$  of 0.0130. However, the lower doses of 50 and 25 µg/mL were statistically nonsignificant, with  $P$  of 0.9085 and 0.9988, respectively (Figure 14).

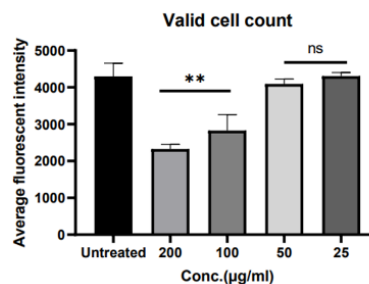


**Figure 14.** L-Met enzyme tested for its effect on CC permeability by assessing the fluorescent intensity

### Pancreatic cancer (PANC-1)

The effects of L-Met on the selected cellular parameters— specifically VCC, TNI, CMP, MMP, and CC— in PANC-1 cells were assessed by Dunnett's multiple comparison tests (Figure 15).

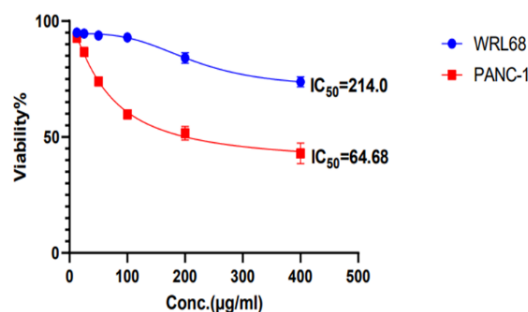


**Figure 15.** Dose-response curves for the L-Met treatment of the normal WRL68 and the PANC-1. Cell viability was assessed after a 24-hour exposure to different concentrations of L-Met (25–500 µg/mL). The  $IC_{50}$  values indicate that the PANC-1 tumor cell line is more sensitive to L-Met compared to the normal WRL-68 cell line, with an  $IC_{50}$  value of 64.68 µg/mL for PANC-1, compared to 214.0 µg/mL for WRL-68. Error bars represent standard deviations from trials conducted in triplicate

A significant dose-dependent reduction in VCC was observed in PANC-1 cells. For instance, the 200 µg/mL dose resulted in a mean difference of 1543 ( $P=0.0031$ ), while the 100 µg/mL dose significantly reduced VCC

**L-methioninase in methionine-dependent cancer therapy**

with a mean difference of 1175 ( $P=0.0096$ ). In contrast, the lower doses of 50  $\mu\text{g/mL}$  and 25  $\mu\text{g/mL}$  did not

exhibit any cytotoxic effect, with  $P$  of 0.7843 and 0.9855, respectively (Table 4).

**Table 4. Dunnett's multiple comparison test results for VCC in PANC-1 cells**

Number of families												
Number of comparisons per family												
Alpha												
Comparison	Mean 1	Mean 2	Mean Diff.	95% CI of Diff.	Below Threshold?	Summary	Adjusted P Value	SE of Diff.	n1	n2	q	DF
Untreated vs. 200 $\mu\text{g/mL}$	3245	1702	1543	813 to 2273	Yes	**	0.0031	272.8	2	2	5.653	5
Untreated vs. 100 $\mu\text{g/mL}$	3245	2070	1175	478 to 1872	Yes	**	0.0096	272.8	2	2	4.307	5
Untreated vs. 50 $\mu\text{g/mL}$	3245	3047	198	-672 to 1068	No	ns	0.7843	272.8	2	2	0.726	5
Untreated vs. 25 $\mu\text{g/mL}$	3245	3233	-12	-882 to 858	No	ns	0.9855	272.8	2	2	0.044	5

In the TNI assay, a similar pattern of cytotoxicity was observed with the same dosage. For the 200  $\mu\text{g/mL}$  dose, the reduction in TNI was substantial, with a mean difference of -179.5 ( $P=0.0011$ ). The 100  $\mu\text{g/mL}$  dose also resulted in a significant reduction, with a mean

difference of -120.0 ( $P=0.0064$ ). However, no significant alterations were observed in TNI at the lower concentrations of 50  $\mu\text{g/mL}$  and 25  $\mu\text{g/mL}$ , which had  $P$  of 0.6352 and 0.8951, respectively (Table 5).

**Table 5. Dunnett's multiple comparison test results for TNI in PANC-1 cells**

Number of families												
Number of comparisons per family												
Alpha												
Comparison	Mean 1	Mean 2	Mean Diff.	95% CI of Diff.	Below Thresh hold?	Summary	Adjusted P Value	SE of Diff.	n1	n 2	q	DF
Untreated vs. 200 $\mu\text{g/mL}$	518.5	339.0	-179.5	-263.0 to -96.0	Yes	***	0.0011	22.30	2	2	8.048	5
Untreated vs. 100 $\mu\text{g/mL}$	518.5	398.5	-120.0	-203.5 to -36.5	Yes	**	0.0064	22.30	2	2	5.383	5
Untreated vs. 50 $\mu\text{g/mL}$	518.5	486.0	-32.5	-116.0 to 51.0	No	ns	0.6352	22.30	2	2	1.459	5
Untreated vs. 25 $\mu\text{g/mL}$	518.5	508.5	-10.0	-93.5 to 73.5	No	ns	0.8951	22.30	2	2	0.448	5

L-Met also influenced cell membrane integrity in PANC-1 cells, as evidenced by a significant decline in CMP of -59.00 at the 200  $\mu\text{g/mL}$  dose, with a p-value of 0.0092. In contrast, the 100  $\mu\text{g/mL}$  concentration did not significantly affect CMP, with a p-value of 0.9793. Similarly, the lower concentrations of 50  $\mu\text{g/mL}$  and 25  $\mu\text{g/mL}$  also showed no significant effects, with  $P$  of

0.9976 and 0.7035, respectively (Table 6).

The highest doses of two L-Met treatments significantly reduced the activity of the key player in cancer metastasis, MMP. The 200  $\mu\text{g/mL}$  dose revealed an average reduction of 279.0 ( $P=0.0037$ ), while the 100  $\mu\text{g/mL}$  dose led to a reduction of 158.5 ( $P=0.0392$ ). In contrast, the lower doses of 50  $\mu\text{g/mL}$  and 25  $\mu\text{g/mL}$  did

not result in significant alterations, with p-values of 0.6663 and 0.8995, respectively (Table 7).

CC analysis showed that a dose of 200 µg/mL of L-Met significantly reduced CC in PANC-1 cells, with a mean difference of -104.5 ( $P=0.0015$ ). A 100 µg/mL dose

also resulted in a significant decline in CC, with a mean difference of -64.50 ( $P=0.0130$ ). However, the 50 µg/mL and 25 µg/mL doses did not exhibit statistical significance, with  $P$  of 0.9085 and 0.9988, respectively (Table 8).

**Table 6. Dunnett's multiple comparison test results for CMP in PANC-1 cells**

Number of families	Number of comparisons per family	Alpha												
			Mean 1	Mean 2	Mean Diff.	95% CI of Diff.	Below Threshold?	Summary	Adjusted P Value	SE of Diff.	n1	n2	q	DF
1	4	0.05												
			176.0	235.0	-59.00	-97.51 to -20.49	Yes	**	0.0092	11.08	2	2	5.326	5
			176.0	180.5	-4.500	-43.01 to 34.01	No	ns	0.9793	11.08	2	2	0.406	5
			176.0	173.5	2.500	-36.01 to 41.01	No	ns	0.9976	11.08	2	2	0.226	5
			176.0	164.5	11.50	-27.01 to 50.01	No	ns	0.7035	11.08	2	2	1.038	5

**Table 7. Dunnett's multiple comparison test results for MMP in PANC-1 cells**

Number of families	Number of comparisons per family	Alpha												
			Mean 1	Mean 2	Mean Diff.	95% CI of Diff.	Below Threshold?	Summary	Adjusted P	SE of Diff.	n1	n2	q	DF
1	4	0.05												
			877.0	598.0	279.0	130.7 to 427.3	Yes	**	0.0037	42.65	2	2	6.541	5
			877.0	718.5	158.5	10.22 to 306.8	Yes	*	0.0392	42.65	2	2	3.716	5
			877.0	830.0	47.00	-101.3 to 195.3	No	ns	0.6663	42.65	2	2	1.102	5
			877.0	848.5	28.50	-119.8 to 176.8	No	ns	0.8995	42.65	2	2	0.668	5

Table 8. Dunnett's multiple comparisons test results for CC in PANC-1 cells

Comparison	Mean 1	Mean 2	Mean Diff.	95% CI of Diff.	Below Threshold?	Summary	Adjusted P	SE of Diff.	n1	n2	q	DF
Number of families	1											
Number of comparisons per family	4											
Alpha	0.05											
Untreated vs. 200 µg/mL	487.5	592.0	-104.5	-150.2 to -58.79	Yes	**	0.0015	13.15	2	2	7.947	5
Untreated vs. 100 µg/mL	487.5	552.0	-64.50	-110.2 to -18.79	Yes	*	0.0130	13.15	2	2	4.905	5
Untreated vs. 50 µg/mL	487.5	479.0	8.500	-37.21 to 54.21	No	ns	0.9085	13.15	2	2	0.646	5
Untreated vs. 25 µg/mL	487.5	485.0	2.500	-43.21 to 48.21	No	ns	0.9988	13.15	2	2	0.190	5

## Discussion

The dependence on L-methionine is a peculiar characteristic often observed in malignantly transformed cells, indicating an essential need for this amino acid in their proliferation. L-Met exploits this weakness of cancer cells by catalyzing the breakdown of L-methionine to  $\alpha$ -ketobutyrate, methanethiol, and ammonia, starving these cells of the amino acid while leaving normal cells unaffected. This finding has been supported by a very recent study that demonstrates the significant cytotoxic effects of L-Met on various cancer cell lines, including HepG2 and PANC-1 (16). Furthermore, recombinant L-Met derived from *Pseudomonas* species has shown increased stability and therapeutic efficacy, particularly when newer delivery systems, such as PEGylation, are employed. PEGylation extends the half-life of the enzyme in the blood while simultaneously lowering its associated immunogenicity (17).

In combination therapies, L-Met has been used synergistically with traditional chemotherapeutics, including doxorubicin, to enhance cytotoxic effects on tumors. It is especially effective against resistant cancer cells, such as those that overexpress anti-apoptotic proteins such as Bcl-2, where its combination with drugs has also elicited significantly improved response (18).

Our results indicated that L-Met exerts a cytotoxic effect on HepG2 cells in a dose-dependent manner. As the concentration of L-Met increased, cell viability significantly declined. The highest concentration tested (200 µg/mL) resulted in a notable decrease in the VCC, with an average difference of 1971 compared to untreated cells. Similarly, the VCC was significantly reduced in the

100 µg/mL group, with a mean difference of 1469 and a p-value of 0.0082. However, no significant effect on cell viability was observed at the lower concentrations of 50 µg/mL and 25 µg/mL. Other cellular parameters, such as TNI and CMP, exhibited a similar trend to VCC, showing significant effects only at higher concentrations of L-Met. The 200 µg/mL dose significantly decreased TNI and CMP, further confirming the dose-dependent cytotoxicity of L-Met against HepG2 cells. However, at lower dosages, no significant changes were observed in these parameters, reinforcing the notion that higher concentrations are more effective. This finding suggests that elevated concentrations of L-Met may be necessary to induce cytotoxicity in HepG2 cells. Hence, this situation establishes L-Met as a potential therapeutic agent capable of targeting specific cancerous cells.

In normal cells, methionine synthase converts homocysteine into methionine using methyl tetrahydrofolate and betaine as methyl group donors (17). However, methionine synthase is either absent or present in trace amounts in methionine-dependent tumor cell lines (19). Previous studies have documented that cancer cell lines rely on methionine synthase more than normal cells (20). L-methionine is essential for biological processes, including the synthesis of vitamins, antioxidants, DNA stabilizers, coenzymes, epigenetic DNA modulators, proteins, and polyamines, which are crucial for healthy cell development. It also plays a vital role in iron-sulfur cluster biosynthesis (energy metabolism), methylation reactions, and antioxidative stress defense (glutathione/trypanothione). Additionally, L-Met regulates gene expression (21).

L-Met is a precursor for cysteine production and the

first amino acid incorporated into many functional proteins following translation. In various animal models, numerous human cancer cell lines and cancer xenografts have been found to be methionine-dependent (22). This dependency is a metabolic abnormality that is unique to cancer cells, which inhibits their proliferation in environments with low methionine levels (23). As a result, L-Met has attracted significant interest as a potential treatment for several kinds of methionine-dependent cancers (24). In our study, L-Met exhibited a cytotoxic effect on PANC-1 cells across all dose-dependent parameters. Notably, it reduced VCC by 1543 at a dose of 200 µg/mL, which was statistically significant at a p-value of 0.0031. A similar reduction in TNI due to the action of the enzyme was observed at -179.5, which was considered significant at  $P=0.0011$ . The enzyme demonstrated comparable reductions in other parameters, such as CMP, MMP, and CC. Notable reductions were also evident at the 100 µg/mL dose for VCC, TNI, and MMP. In contrast, lower doses of 50 µg/mL and 25 µg/mL did not significantly impact any of the parameters; therefore, higher concentrations of L-Met are necessary for a meaningful induction of cytotoxic response in PANC-1 cells. These findings underscore the potential of the enzyme as a targeted anticancer agent against PANC-1.

The Warburg effect, which describes an increased dependence on glucose through glycolysis and is frequently observed in malignant cells, was demonstrated by cancer cells (25). Facilitative glucose transporter (GLUT) proteins are essential for glucose transport, which is the rate-limiting step of glucose metabolism in cells. Cancer cells absorb more glucose than normal cells because their sugar transporters become active. Among the various transporters, glucose transporters (GLUTs) and sodium-dependent glucose transporters (SGLT) play crucial roles in tumor cells, where membrane transporters and channel proteins enhance uptake from external sources and endogenous synthesis increases (26). The expression of the sodium-glucose symporter SGLT2, one of the SGLT transporters, was considerably higher in the liver and lymph nodes (27). Additionally, fatty acid production and glutamine metabolism rates are elevated in tumors. Human HepG2, oral cancer, the human PANC-1 cell line (28), and MKN45 (human gastric cancer) have all been shown to express GLUT1 at high levels. Active transport through SGLT or facilitated diffusion via GLUT enables glucose to cross the cell membrane (29). Thus, the efficacy of widely used medicinal drugs is enhanced by cellular metabolic enzymes, including glucose transporters, hexokinase, pyruvate kinase, lactate

dehydrogenase, pyruvate dehydrogenase kinase, fatty acid synthase, and glutaminase. The overexpression of GLUT-1 has been shown to increase the activity of the MMP-2 promoter and facilitate the binding of p53 to the MMP-2 promoter (30). Glutamate transport is mediated by solute carrier family A1 member 5 (SLC1A5), which has been overexpressed and linked to squamous lung cancer (31). Fatty acids are transported by the carnitine palmitoyltransferase 1 transporter as acyl-CoA and subsequently converted to acetyl-CoA. Acetyl-CoA enters the tricarboxylic acid cycle through oxidative phosphorylation, generating NADH, which provides energy for the cell (32).

Further research into gene therapy advancements has led to the development of adenoviral vectors that introduce the methioninase gene to tumor cells, increasing local expression of the enzyme and amplifying its therapeutic effects. This approach is complemented by the use of agents such as selenomethionine, which induce oxidative stress and apoptosis in tumor cells, enhancing treatment outcomes. Despite these promising results, challenges remain in identifying effective delivery systems, managing potential side effects, and refining the therapeutic window to maximize efficacy while minimizing harm to normal tissues. However, ongoing developments in recombinant technology, nanoparticle delivery systems, and combination therapies suggest a promising future for L-Met as a new cancer treatment strategy.

Our findings highlight the significant potential of L-Met as a selective anticancer agent, with its effects demonstrating a clear dose-dependent relationship. Higher concentrations of L-Met exhibited substantial cytotoxicity toward HepG2 and PANC-1 tumor cells, as evidenced by reductions in VCC, TNI, and CMP. These changes indicate that L-Met effectively induces cell death in methionine-dependent tumor cells. However, there was no noticeable cytotoxicity at lower concentrations, highlighting that the therapeutic efficacy of L-Met is closely tied to its concentration. This dose-dependent behavior emphasizes the importance of optimizing L-Met dosage in cancer therapies, particularly for tumors reliant on methionine, offering a promising avenue for targeted cancer treatments.

## Acknowledgments

The authors thank the University of Babylon, for their generous support in providing necessary laboratory equipment and facilitating suitable facilities.

## References

1. Javia BM, Gadhvi MS, Vyas SJ, Ghelani A, Wirajana N, Dudhagara DR. A review on L-methioninase in cancer therapy: Precision targeting, advancements and diverse applications for a promising future. *Int J Biol Macromol* 2024;130997.
2. Bu T, Lan J, Jo I, Zhang J, Bai X, He S, et al. Structural Basis of the Inhibition of L-Methionine  $\gamma$ -Lyase from *Fusobacterium nucleatum*. *Int J Mol Sci* 2023;24:1651.
3. Wise DR, Thompson CB. Glutamine addiction: a new therapeutic target in cancer. *Trends Biochem Sci* 2010;35:427-33.
4. Halpern BC, Clark BR, Hardy DN, Halpern RM, Smith RA. The effect of replacement of methionine by homocystine on survival of malignant and normal adult mammalian cells in culture. *Proc Natl Acad Sci* 1974;71:1133-6.
5. Cellarier E, Durando X, Vasson M, Farges M, Demiden A, Maurizis J, et al. Methionine dependency and cancer treatment. *Cancer Treat Rev* 2003;29:489-99.
6. Kubota Y, Han Q, Aoki Y, Masaki N, Obara K, Hamada K, et al. Synergy of combining methionine restriction and chemotherapy: the disruptive next generation of cancer treatment. *Cancer Diagn Progn* 2023;3:272.
7. Tan Y, Xu M, Hoffman RM. Broad selective efficacy of recombinant methioninase and polyethylene glycol-modified recombinant methioninase on cancer cells in vitro. *Anticancer Res* 2010;30:1041-6.
8. Kawaguchi K, Igarashi K, Li S, Han Q, Tan Y, Miyake K, et al. Recombinant methioninase (rMETase) is an effective therapeutic for BRAF-V600E-negative as well as-positive melanoma in patient-derived orthotopic xenograft (PDOX) mouse models. *Oncotarget* 2018;9:915.
9. Sundar WA, Nellaiah H. Production of methioninase from *Serratia marcescens* isolated from soil and its anti-cancer activity against Dalton's Lymphoma Ascitic (DLA) and Ehrlich Ascitic Carcinoma (EAC) in swiss albino mice. *Trop J Pharm Res* 2013;12:699-704.
10. Sorin M, Watkins D, Gilfix BM, Rosenblatt DS. Methionine dependence in tumor cells: The potential role of cobalamin and MMACHC. *Mol Genet Metab* 2021;132:155-61.
11. Pokrovsky VS, Abo Qoura L, Demidova EA, Han Q, Hoffman RM. Targeting methionine addiction of cancer cells with methioninase. *Biochemistry* 2023;88:944-52.
12. Dayanand K, Nadumane VK. Effect of physicochemical parameters on the L-methioninase activity of *Methylobacterium* sp. and its in vitro anticancer activity in combination with tamoxifen citrate. *Futur J Pharm Sci* 2023;9:94.
13. Zou Y, Yuan Y, Zhou Q, Yue Z, Liu J, Fan L, et al. The Role of Methionine Restriction in Gastric Cancer: A Summary of Mechanisms and a Discussion on Tumor Heterogeneity. *Biomolecules* 2024;14:161.
14. Zhao T, Lum JJ. Methionine cycle-dependent regulation of T cells in cancer immunity. *Front Oncol* 2022;12:969563.
15. Sedillo JC, Cryns VL. Targeting the methionine addiction of cancer. *Am J Cancer Res* 2022;12:2249.
16. Aldawood AS, Al-Ezzy RM. Cytotoxicity of L-Methioninase Purified from Clinical Isolates of *Pseudomonas* Species in Cancer Cell Lines. *Al-Rafidain J Med Sci* 2024;6:46-9.
17. Qoura LA, Balakin KV, Hoffman RM, Pokrovsky VS. The potential of methioninase for cancer treatment. *BBA Reviews on Cancer* 2024:189122.
18. Muharram MM. Recombinant Engineering of L-Methioninase Using Two Different Promoter and Expression Systems and in vitro Analysis of Its Anticancer Efficacy on Different Human Cancer Cell Lines. *Pak J Biol Sci* 2016;19:106-14.
19. Hoffman R. Altered methionine metabolism and transmethylation in cancer. *Anticancer Res* 1985;5:1-30.
20. El-Sayed AS. Microbial L-methioninase: production, molecular characterization, and therapeutic applications. *Appl Microbiol Biotechnol* 2010;86:445-67.
21. Davis CD, Uthus EO. DNA methylation, cancer susceptibility, and nutrient interactions. *Exp Biol Med* 2004;229:988-95.
22. Eymard N, Bessonov N, Volpert V, Kurbatova P, Gueyffier F, Nony P. Pharmacokinetic/pharmacodynamic model of a methionine starvation based anti-cancer drug. *Med Biol Eng Comput* 2023;61:1697-722.
23. Guo H-Y, Herrera H, Groce A, Hoffman RM. Expression of the biochemical defect of methionine dependence in fresh patient tumors in primary histoculture. *Cancer Res* 1993;53:2479-83.
24. Kokkinakis DM, Schold Jr SC, Hori H, Nobori T. Effect of long-term depletion of plasma methionine on the growth and survival of human brain tumor xenografts in athymic mice. *Nutr Cancer* 1997;29:195-204.
25. Zhao Y, Butler EB, Tan M. Targeting cellular metabolism to improve cancer therapeutics. *Cell Death Dis* 2013;4:e532-e.
26. Calvo MB, Figueroa A, Pulido EG, Campelo RG, Aparicio LA. Potential role of sugar transporters in cancer and their relationship with anticancer therapy. *Int J Endocrinol* 2010;2010:205357.
27. Ishikawa N, Oguri T, Isobe T, Fujitaka K, Kohno N. SGLT gene expression in primary lung cancers and their

- metastatic lesions. *Jpn J Cancer Res* 2001;92:874-9.
28. Younes M, Lechago LV, Somoano JR, Mosharaf M, Lechago J. Wide expression of the human erythrocyte glucose transporter Glut1 in human cancers. *Cancer Res* 1996;56:1164-7.
  29. McCracken AN, Edinger AL. Nutrient transporters: the Achilles' heel of anabolism. *Trends in Endocrinology & Metabolism* 2013;24:200-8.
  30. Ito S, Fukusato T, Nemoto T, Sekihara H, Seyama Y, Kubota S. Coexpression of glucose transporter 1 and matrix metalloproteinase-2 in human cancers. *J Natl Cancer Inst* 2002;94:1080-91.
  31. Hassanein M, Hoeksema MD, Shiota M, Qian J, Harris BK, Chen H, et al. SLC1A5 mediates glutamine transport required for lung cancer cell growth and survival. *Clin Cancer Res* 2013;19:560-70.
  32. Macheda ML, Rogers S, Best JD. Molecular and cellular regulation of glucose transporter (GLUT) proteins in cancer. *J Cell Physiol* 2005;202:654-62.